ISSN 1064-2269, Journal of Communications Technology and Electronics, 2018, Vol. 63, No. 7, pp. 721–731. © Pleiades Publishing, Inc., 2018.
Original Russian Text © G.A. Kraftmakher, V.S. Butylkin, Yu.N. Kazantsev, V.P. Mal'tsev, 2018, published in Radiotekhnika i Elektronika, 2018, Vol. 63, No. 7, pp. 641–651.

ELECTRODYNAMICS AND WAVE PROPAGATION

Electrically and Optically Controlled Wideband Matching of Radio-Absorbing Composites to the Ambient Space

G. A. Kraftmakher[a], *, V. S. Butylkin[a], Yu. N. Kazantsev[a], and V. P. Mal'tsev[a]

[a] *Institute of Radio Engineering and Electronics (Fryazino Branch), Russian Academy of Sciences, Fryazino, Moscow oblast, 141190 Russia*

**e-mail: gkraft@ms.ire.rssi.ru*

Received October 19, 2016

Abstract—Microwave radio-absorbing metastructures are proposed that possess controlled broadband matching to the ambient space by virtue of an array of varactor-loaded chiral and annular elements in which magnetic resonance are excited. Experimentally in a rectangular waveguide and numerically in free space, it is shown that the tuning of the magnetic resonance frequency leads to a shift in the matching frequency region. The electric control of the magnetic resonance and, accordingly, the matching (25% relative tuning) is achieved by the variation in the reverse bias voltage at the varactor, and the optical control is achieved by directing a red laser pointer to a photodiode connected to the varactor in the photodiode mode.

DOI: 10.1134/S1064226918070082

INTRODUCTION

It is known that the key task in the problem of electromagnetic-wave absorption is the matching of the radio absorber to the ambient space in order to compensate the reflections. Traditionally, it was achieved by choosing resonant types of absorbers based on quarter-wave effects, or by reaching close permittivity and permeability, or by using a matching quarter-wave layer from a nonabsorbing material.

There are radio-absorbing metastructures with the matrices incorporating conducting chiral inclusions, responsible for the permeability, or other resonance elements on which the permittivity and, accordingly, the frequency range and the absorption and reflection levels depend substantially [1, 2].

The control of the resonance in conducting chiral and dipole elements opens wide possibilities for the development of metastructures with predefined properties for various kinds of electromagnetic-wave propagation (free space, waveguides). Electrical control of selectively reflecting and transmitting structures, as well as nonreciprocal ones, was investigated using rectangular waveguides [3–6].

The use of conducting chiral and resonant elements expands and opens new functional possibilities of composite radio-absorbers. They include the electrical control of absorption due to the possibility of fast adjustment of the resonance properties of individual inclusions by relatively simple means. For this purpose, varactors, whose capacitance can be changed by applying a reverse bias voltage, are introduced into the discontinuities of the elements or between elements [7–12]. Controlled radio-absorbing composites are in demand in radiolocation, communication technology, measuring technology, etc., and, therefore, they attract much attention. In this paper, we propose and implement a controlled matching of radio-absorbing composites. Chiral inclusions are used not as components embedded in the absorber matrix but as a matching layer [13, 14]. Their magnetic response can be used not only to create artificial composites with magnetic properties [15] but also for broadband matching of radio-absorbing composites on the basis of resistive filaments or films. The matching is realized due to the achievement of close but antiphase reflection from the composite and an array of closely spaced resonant elements excited by the magnetic field of the wave. On the basis of measurements in rectangular microwave waveguides, the electrical and optical control of both the magnetic resonance and the associated resonance matching of the corresponding radio-absorbing metastructures is studied. The possibility of such control was demonstrated in [16].

1. CONTROLLED MATCHING ELEMENTS AND RADIO-ABSORBING METASTRUCTURES

In this work, we study several different elements made of a copper planar double split-ring resonator (PDSRR) (Fig. 1a) and used for controlled matching of microwave radio absorbers: a PDSRR with an additional gap in the outer ring, where a stationary capacitor with the necessary capacitance is soldered (Fig. 1b) or a MA46H120 (MACOM) varactor, which

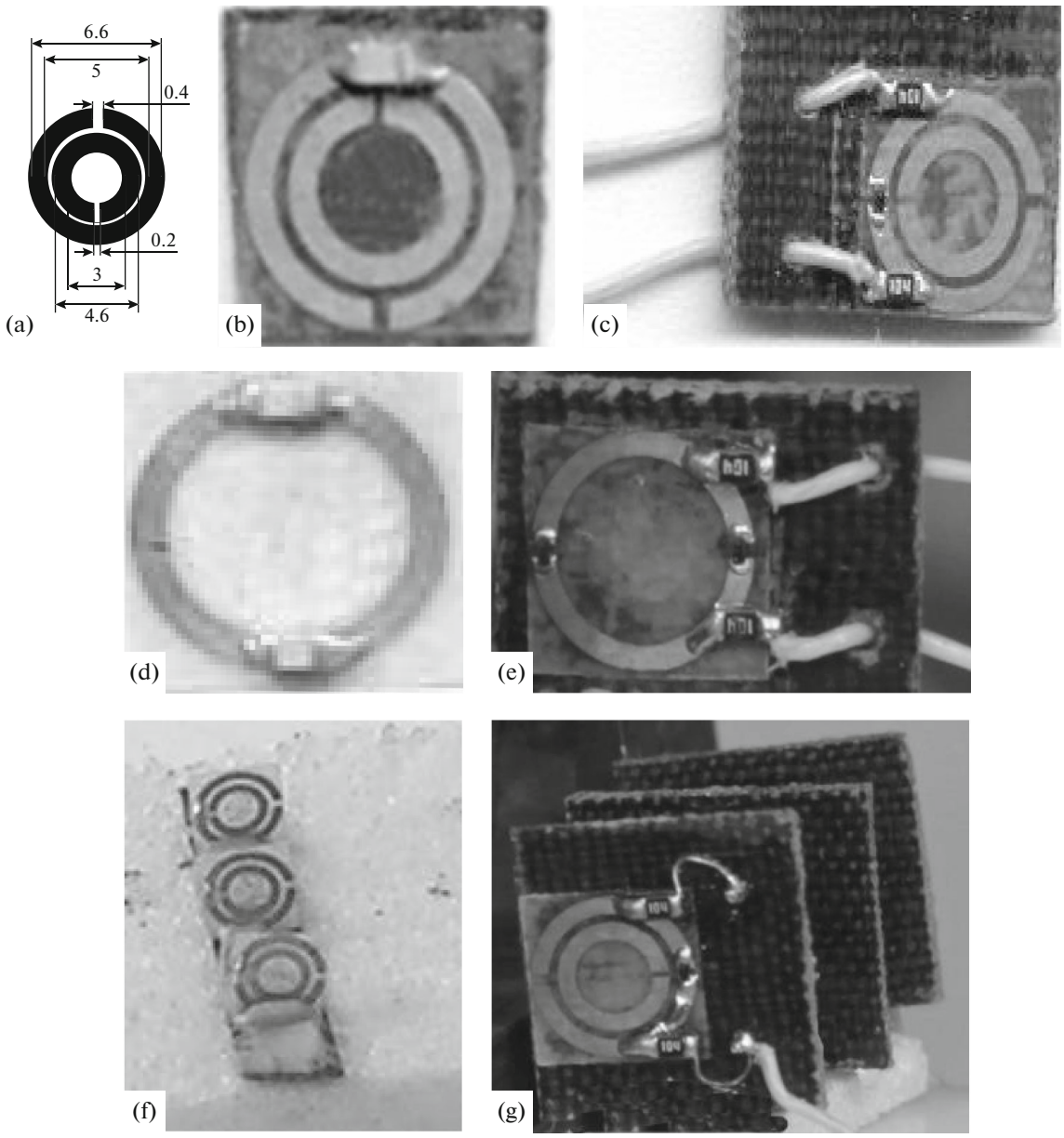

Fig. 1. Elements under study: (a) schematic of a planar double-split-ring resonator (PDSRR); (b) a PDSRR with a capacitance in an additional gap of the outer ring; (c) a PDSRR with a MA46H120 (MACOM) varactor in an additional gap in the outer ring; (d) a single symmetrically-twice-split-ring resonator (STSRR) loaded with capacitances; (e) an STSRR with two varactors in the gaps; (f) a series of three PDSRRs with capacitances in the outer gap; (g) a series of three PDSRRs with varactors.

has an electrically controlled capacitance ranging from 1 to 0.15 pF as the reverse bias voltage is varied from 0 to 29 V (Fig. 1c); a single twice-split ring resonator (STSRR), to the two gaps of which two stationary capacitances (Fig. 1d) or two varactors (Fig. 1e) are soldered; and a series of three PDSRRs with an additional gap loaded with a capacitance (Fig. 1f) or a varactor (Fig. 1g).

For measurements in a rectangular waveguide, radio-absorbing metastructures comprising a layered absorber and various densely placed matching annular elements were made: a PDSRR with a capacitance in an additional gap (Fig. 2a), single split-ring resonators with two capacitances in two gaps (Fig. 2b), a PDSRR with a varactor in the additional gap (Fig. 2c), and a single split-ring resonator with two varactors in two gaps (Fig. 2d).

2. EXPERIMENTAL

A technique based on measurements of the reflection coefficients R in a rectangular waveguide in the

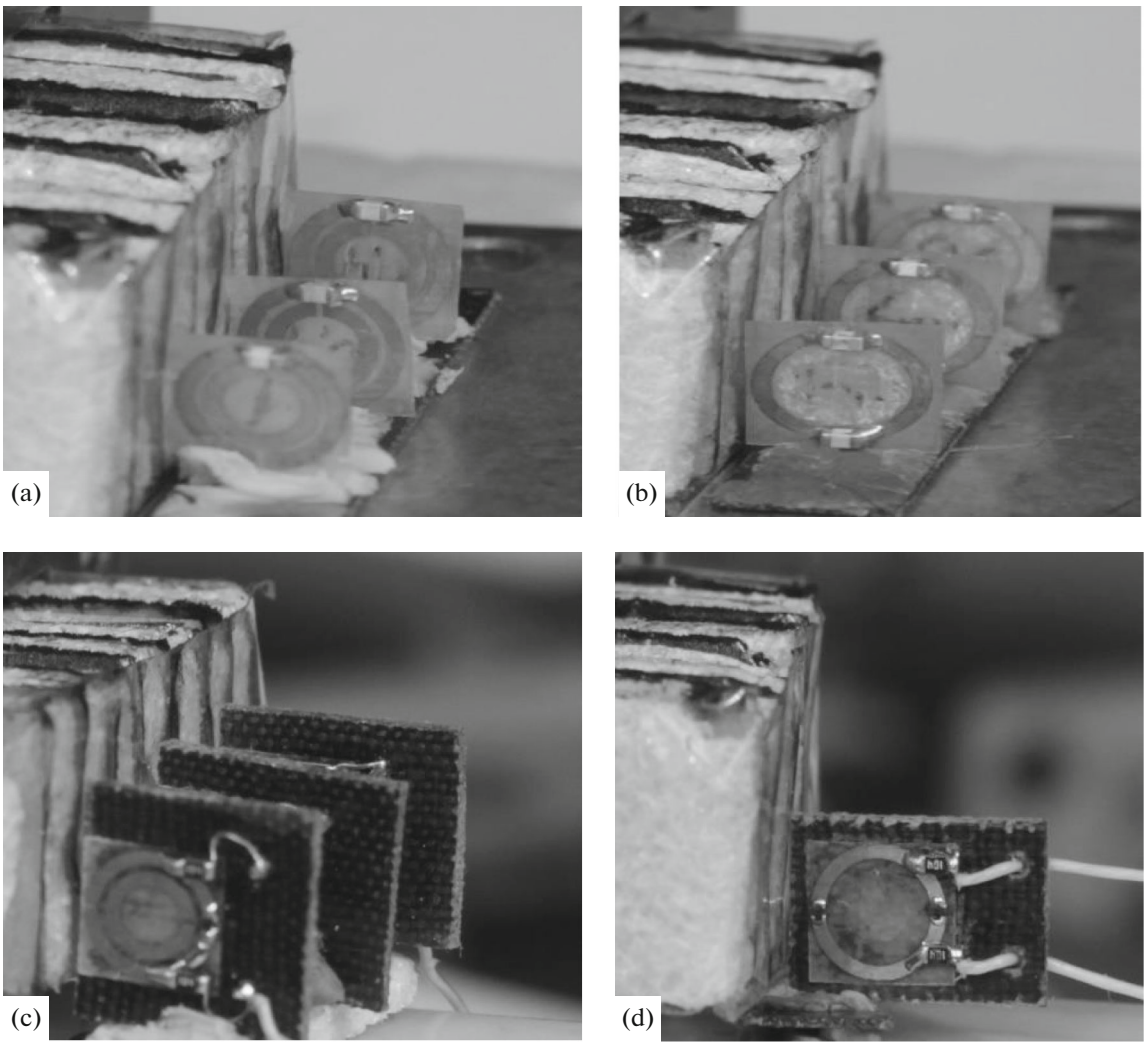

Fig. 2. Controllable absorbing composites with matching elements of different form: (a) a PDSRR with a capacity in an additional gap in the outer ring; (b) an STSRR with capacitances in symmetric gaps; (c) a PDSRR with a varactor in an additional gap in the outer ring; (d) an STSRR with two varactors in symmetric gaps.

traveling-wave mode (with a matched load) and R_m in the standing-wave mode (with a metal plug) is proposed. We used R2-58 meters of voltage standing wave ratio, a 48 × 24 mm waveguide (3–5.5 GHz), R2-59, and a 35 × 15 mm waveguide (5.3–7.6 GHz). The ring resonator (a row of ring resonators) under study was placed along the direction of the wave propagation and was oriented for the excitation of a magnetic resonance (MR), in which the microwave magnetic field h of the incident wave is directed along the axis of the ring, inducing resonance ring currents. Then, the MR region was detected and the control of the reflection characteristics R and R_m was studied by measuring the variation in the frequency dependences by the replacement of stationary capacitances in the gaps of the rings or by varying the capacitance of the varactor by applying a reverse bias voltage in the electric control. The radio-absorbing metastructure with matching ring resonators was placed into a waveguide, the frequency regions of the matching to the ambient space were found, and the possibilities of control were examined by analyzing the coupling with the controlled MR.

For the optical control, we used a photodiode in combination with a varactor in the photodiode mode. In [17], the photovoltaic mode (without an external power source) was used for the optical control of the magnetic resonance, when a voltage dependent on the radiation flux and load appeared on the terminals of the photodiode under the action of light. The photodiode operated as a solar battery, supplying the varactor with a reverse bias voltage V_{rb}. In this work, we used the photodiode mode when a power supply biasing the photodiode in the opposite direction is needed. In this case the reverse current flowing through the photodiode is proportional to the light flux and provides an

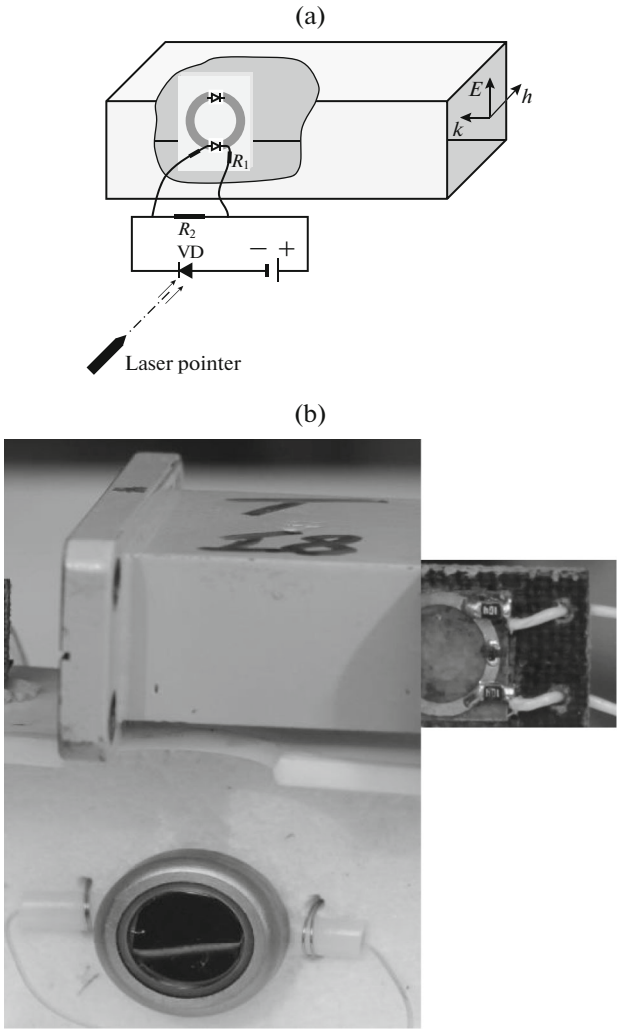

Fig. 3. (a) Schematic and (b) photo of a measuring cell on the basis of a rectangular waveguide for optical control on the example of an STSRR with varactors in combination with a photodiode in the photodiode mode.

appropriate voltage drop on the load and reverse bias on the varactor. In the absence of light, the reverse current does not depend on the reverse voltage applied. The photodiode mode provides a faster response and, as shown in this work, the efficiency of the control is not worse than with a purely electric control of the varactors.

Figure 3a shows the scheme of measuring the characteristics of the MR on the example of a single twice-split ring resonator (STSRRs) with two varactors connected to the gaps. The ring is located in the waveguide, and the YD photodiode, the power source, and the load R_2 are outside of the waveguide. The role of a light source was played by a red laser pointer, located a few meters away from the photodiode. To exclude the excitation of parasitic resonances, the resistor of R_1 = 100 kΩ was used, and the supply wires were perpendicular to the microwave electric field E. The load R_2 = 10 kΩ was chosen in accordance with the maximum shift of the resonance frequency when the photodiode was illuminated. Figure 3b shows a waveguide section in which a split-ring resonator with varactors is placed, and a photodiode is outside of the waveguide.

3. ELECTRICALLY AND OPTICALLY CONTROLLED MAGNETIC RESONANCE

3.1. Planar Double Split-Ring Resonators with an AdditionalGap in the Outer Ring

For the analysis of PDSRRs, the frequency spectra of reflection coefficient R in the traveling-wave mode and R_m in the standing-wave mode were recorded. The MR frequency region was determined by identifying the type of resonance: magnetic, electric, or dipole, from the distinctive features of R, proposed in [13]. Figure 4a shows the measured frequency dependences of R in the MR region for two structures from three PDSRRs. A capacitance of 1 pF was introduced into the additional gap in the first case and, of 0.1 pF, in the second case. We see that the change in the capacitance leads to a shift of the resonance maximum and minimum of R, while the distinctive features typical of the MR (the minimum at a lower frequency than the frequency of the maximum and a high reflection level above the maximum) are preserved. Figures 4b and 4c show the frequency dependences of R and R_m for varactor-loaded PDSRRs. We can clearly see an electrically controlled displacement of the resonance minimum and maximum of R, as well as of the resonance dip of R_m when the capacitance is adjusted by varying the reverse bias voltage V_{rb} from 0 to 20 V. The corresponding arrangement of the elements is shown in Figs. 4a–4c to the right of the plots.

The optically controlled magnetic resonance (based on the measurements by the scheme shown in Fig. 3 and the procedure described in Section 2) is demonstrated in Figs. 4d and 4e. The frequency dependences of R_m in the MR region are presented: in the absence of light, regardless of the applied voltage V_{rb} (Fig. 4d, curve *1*), and with light switched on and V_{rb} = 15 V (curve *2*). While directing the radiation from a red laser pointer (7 kL) to the photodiode, a shift in the resonance frequency, which depends on V_{rb}, was observed (see Fig. 4e).

3.2. Single Twice-Split-Ring Resonators

Similar measurements were made for single twice-split-ring resonators (see Figs. 1d and 1e). Figure 5 shows the experimental frequency dependences of R and R_m in the MR region for a single twice-split-ring resonator: R in the case of free gaps (Fig. 5a) and gaps

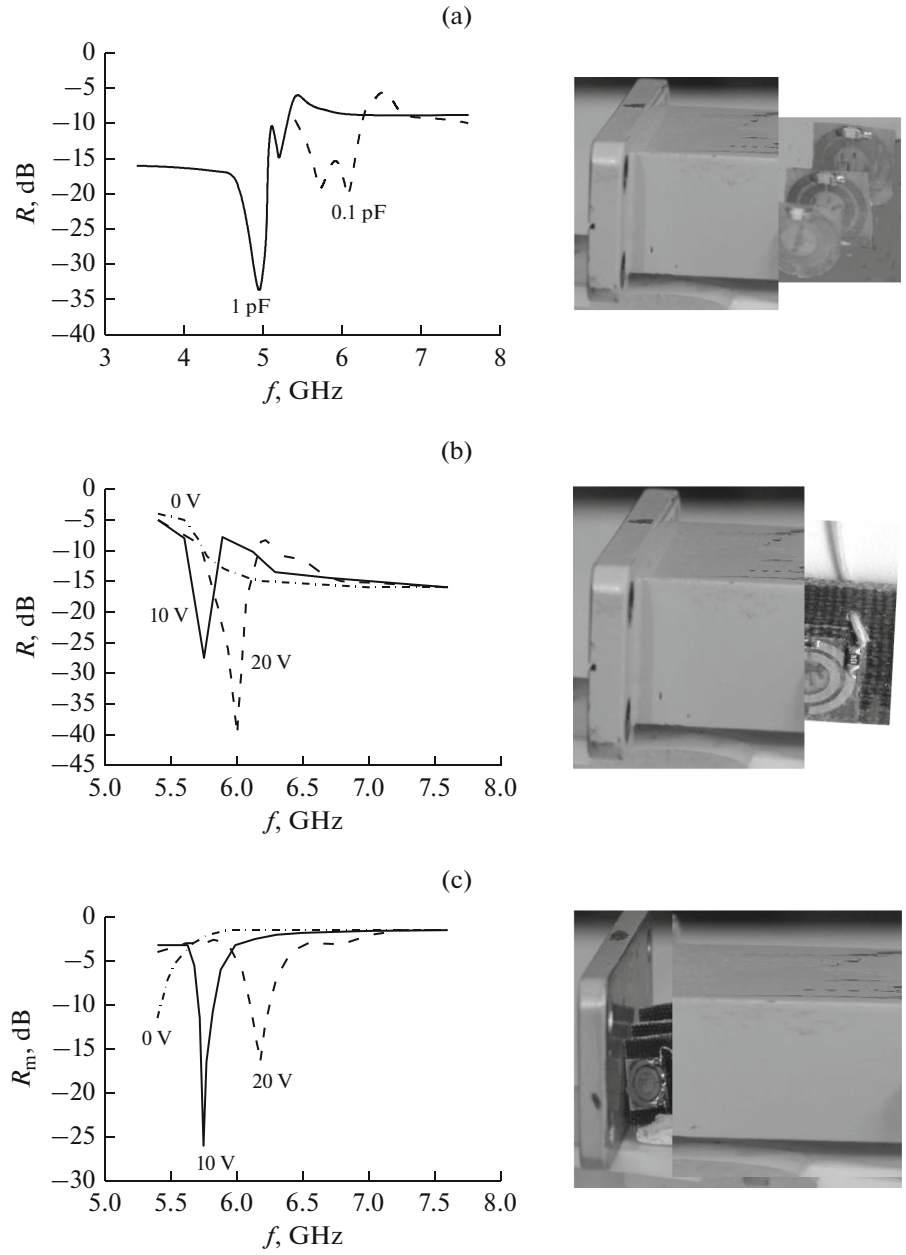

Fig. 4. Dynamics of the experimental frequency dependences of the reflection coefficients (a, b) R and (c, d, e) R_m in the region of an MR from three PDSRR with variation in the capacitances in the additional gap: (a) capacitances of 0.1 and 1 pF; (b) electric control, varactor, $V_{rb} = 0$, 10 and 20 V; (c) varactor, $V_{rb} = 0$, 10 and 20 V; (d) optical control, varactor/photodiode, $V_{rb} = 15$ V, (*1*) in the absence of light and (*2*) under illumination; (e) the resonance frequency (the photodiode is illuminated) vs. voltage V_{rb}.

loaded with two capacitances of 0.1 pF (Fig. 5b); an electrically controlled reflection coefficient R and the reflection coefficient R_m in the case of gaps loaded with two varactors (Figs. 5c and 5d), and an optically controlled R_m in the case of gaps loaded with two varactors in combination with a photodiode (Fig. 5e). To the right of each graph, the corresponding arrangement of the element is shown. It can be seen that the addition of a capacitance in the gap leads to a shift in the resonance maximum and minimum of R with preserving the shape of the resonance curve that distinguishes an MP from a dipole resonance. The introduction of varactors leads to the possibility of electrical control, and the combination of varactors with a photodiode makes it possible to control the resonance characteristics of reflection by turning light on and off. In the absence of light, the reflection coefficient R_m (Fig. 5d, curve *1*) does not depend on V_{rb}. Directing light to the photodiode, we obtain dips of the reflection coefficient R_m at different frequencies, depending on the applied

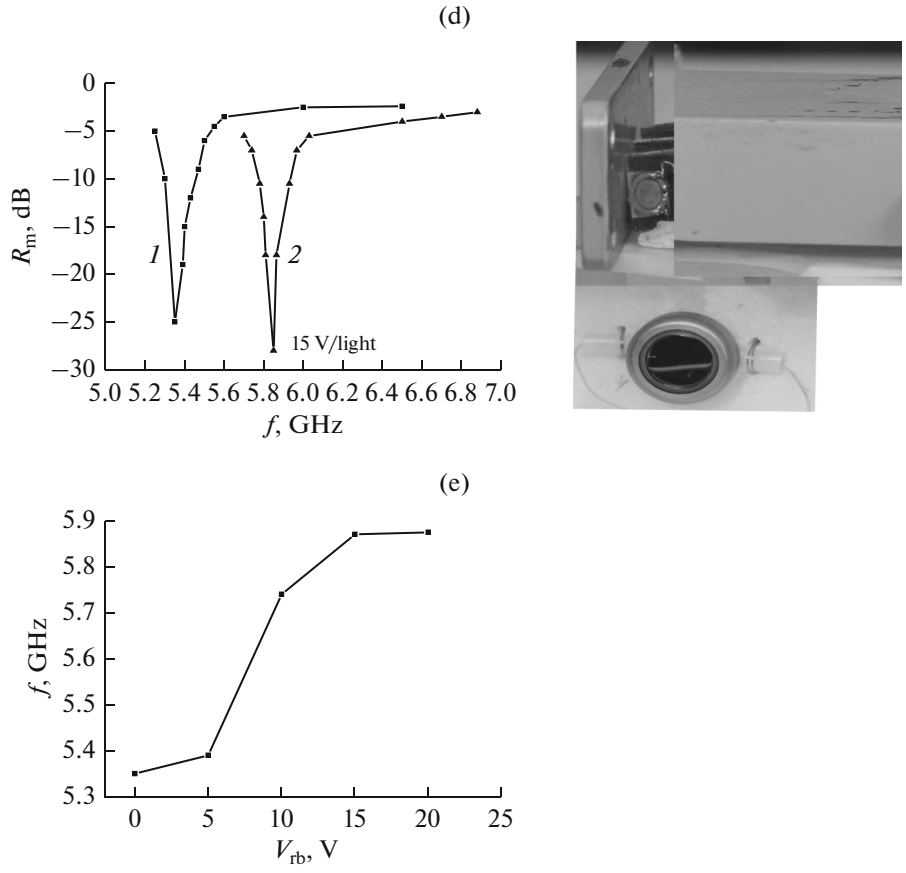

Fig. 4. (Contd.)

voltage V_{rb} (curves *2–5*): f (4 V/light) = 3.48 GHz, f (7 V/light) = 4 GHz, f(9 V/light) = 4.5 GHz, and f (14 V/light) = 4.8 GHz.

Figure 6 shows the results of calculating the absolute value and phase of R of single split-ring resonators with free gaps (curve *1*) and with different capacitances inserted to the gaps (curves *2–5*). Two resonance effects appear in the spectrum of R. The first is a magnetic resonance with a maximum of the reflection coefficient R, which corresponds to a dip of the transmission coefficient T at 12.9 GHz and a minimum of R at 10.6 GHz; both are shifted towards low frequencies with increasing capacitance while their mutual position, characteristic of an MR, is preserved. The second resonance is identified as a dipole one (DR) from the relationship between the maximum and minimum of R, characteristic of the electric excitation: there is a maximum of reflection corresponding to the dip of the transmission coefficient T at 16 GHz and a minimum at a higher frequency near 18 GHz. In the case of symmetrically split ring resonator, electric excitation causes a DR, since the ring current can be induced only by a magnetic field. We see that the DR is not displaced when the capacity is changed. In addition, in an MR, the phase of R varies smoothly, passing through zero, and when the resonance shifts, this feature of the MR persists, while, in a DR, the phase changes abruptly. The features of an MR are very important for matching the composite, since they make it possible to provide close values of antiphase reflection from the composite and closely located array of resonant elements excited by the magnetic field.

4. CONTROLLED MATCHING OF RADIO-ABSORBING COMPOSITES

Thanks to the use of varactor-loaded chiral PDSRRs and magnetically excited STSRRs as matching elements of absorbers, efficient electrical and optical control was achieved.

Figure 7 shows the dependence of R—measured in a rectangular waveguide in the frequency domain of the matching to free space—for a radio-absorber with a matching layer of three PDSRRs oriented under a magnetic excitation (curves *1'–3'*) in comparison with the R of a free absorber (curves *1*) on the capacitance in the additional gap of the outer ring. The results were obtained for a PDSRR with a constant capacitance (Fig. 7a), a varactor (Fig. 7b), and a varactor in com-

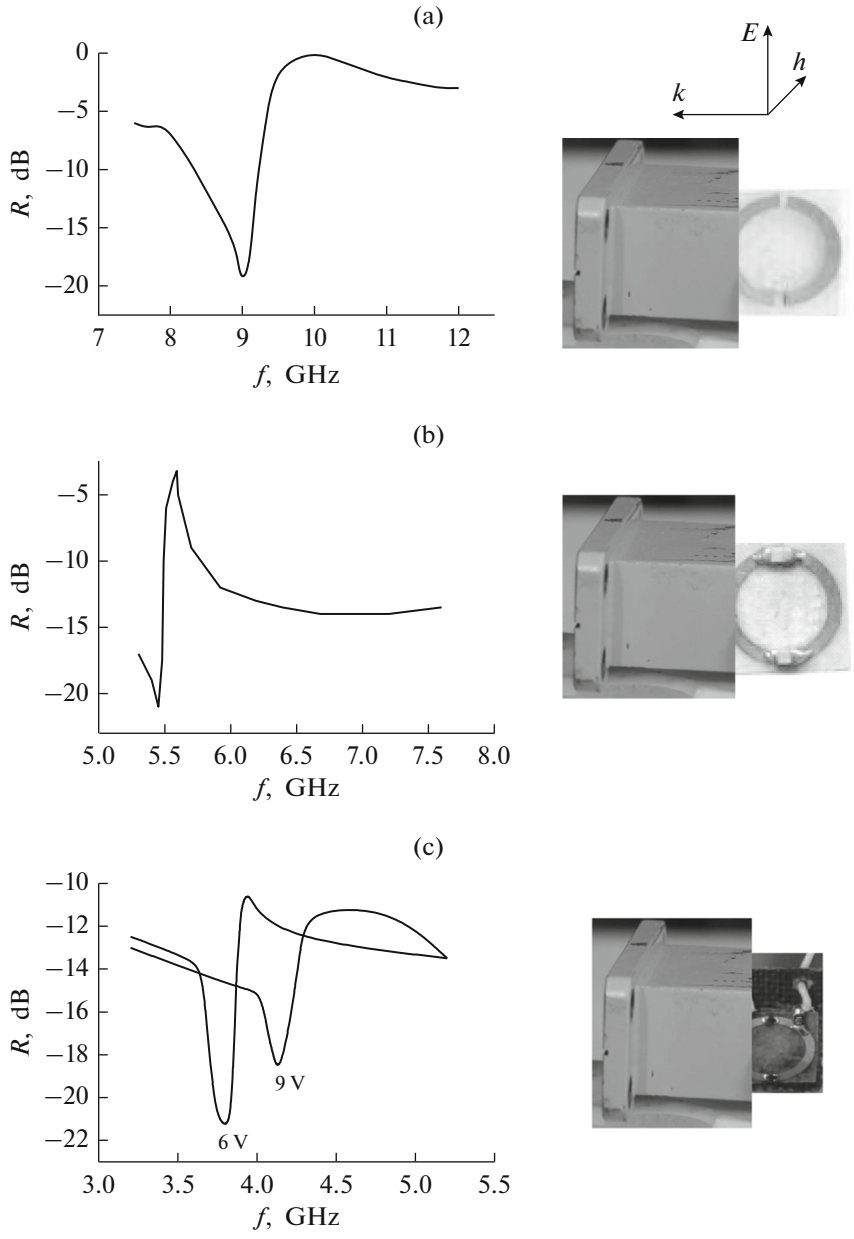

Fig. 5. Dynamics of the experimental frequency dependences of the reflection coefficients (a, b, c) R and (d, e) R_m in the region of an MP from an STSRR upon variation in the capacitances in the gaps: (a) free gaps; (b) capacitances of 0.1 pF; (c) two varactors, $V_{rb} = 6$ and 9 V (electrical control); (d) two varactors, $V_{rb} = 5$, 7, and 15 V; (e) two varactors/photodiode (optical control) (*1*) in the absence of light and (*2*) under illumination, $V_{rb} =$ (*2*) 4, (*3*) 7, (*4*) 9, and (*5*) 14 V.

bination with a photodiode (Fig. 7c). In the figures, we see wide dips in the reflection coefficient, which correspond to the matching frequency regions; they shift when the capacitance of 0.1 pF is replaced by 1 pF (see Fig. 7a). The dips are electrically retuned by varying the reverse bias voltage on the varactor: for example, at $V_{rb} = 0$, the dips are observed at frequencies of 4.4 and 6 GHz and, at $V_{rb} = 10$ V, at 5.15 and 6.3 GHz (see Fig. 7b). The relative adjustment is 20–30%.

In Fig. 7c, it is shown that, if a varactor is used in a circuit with a photodiode, as in Fig. 3a, the matching regions can be controlled by turning on and off the light from a red laser pointer directed to the photodiode. It is seen that the frequency dependence of R with a dip at 6.2 GHz in the absence of light does not depend on V_{rb} (curve *1*'). However, when the photodiode is illuminated, the characteristic R varies depending on the applied voltage V_{rb} (5 V/light corresponds to

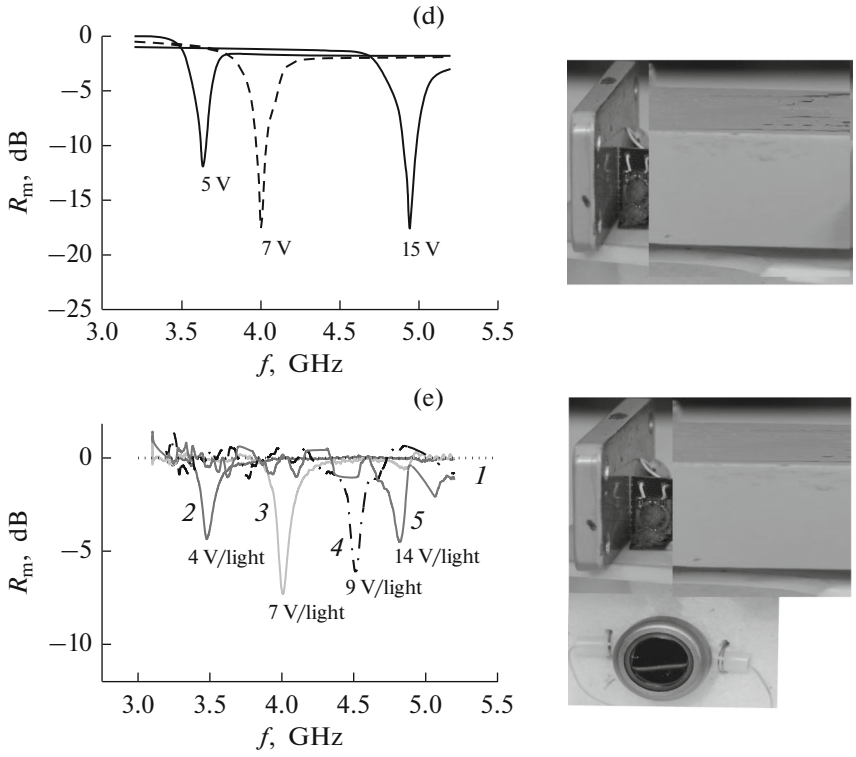

Fig. 5. (Contd.)

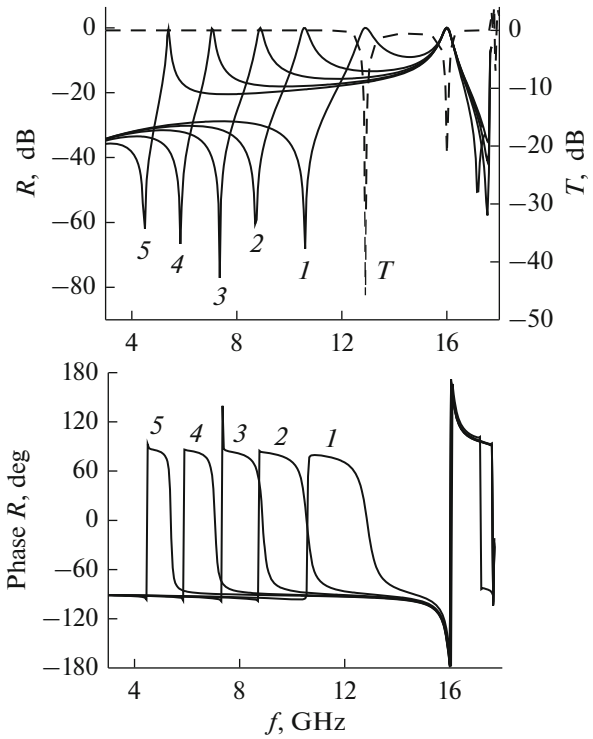

Fig. 6. Calculated dependences of the reflection coefficients R ((a) the absolute value and (b) phase) and (a) transmission coefficient T for a periodic array (the period of the array is 13 mm) of STSRRs in free space (*1*) with free gaps and at different capacitances in the gaps of (*2*) 0.018, (*3*) 0.035, (*4*) 0.07, and (*5*) 0.14 pF.

V_{rb} = 5 V (curve *2*'), and 15 V/light corresponds to V_{rb} = 15 V (curve *3*')).

Similar experiments were conducted for a matching symmetrically-twice-split-ring resonator loaded with two varactors (Fig. 8a) and varactors in combination with a photodiode (Fig. 8b). Figure 8a shows the broadband compensation of the reflection coefficient R with the dips (curve *1*') and electrical control with frequency tuning upon application of V_{rb} = 5 and 9 V. Figure 8b demonstrates the optical control. At 5 GHz, a dip of R appears, which, in the absence of light, does not depend on V_{rb} (curve *1*'). However, when the photodiode is illuminated, the reflection characteristic changes: the dip shifts in frequency and an additional dip appears at 4 GHz at V_{rb} = 6 V (6 V/light, curve *2*'), which shifts to 4.5 GHz at V_{rb} = 8 V (8 V/ curve *3*'). It can be concluded that the optical control is not inferior to purely electrical in the degree of variation in the reflection characteristics.

Figure 8c shows the calculation results confirming the possibility of control of reflection dips in the matching region by varying the capacitance in the gaps of STSRRs.

CONCLUSIONS

Thus, microwave radio-absorbing metastructures the matching of which to the ambient space can be

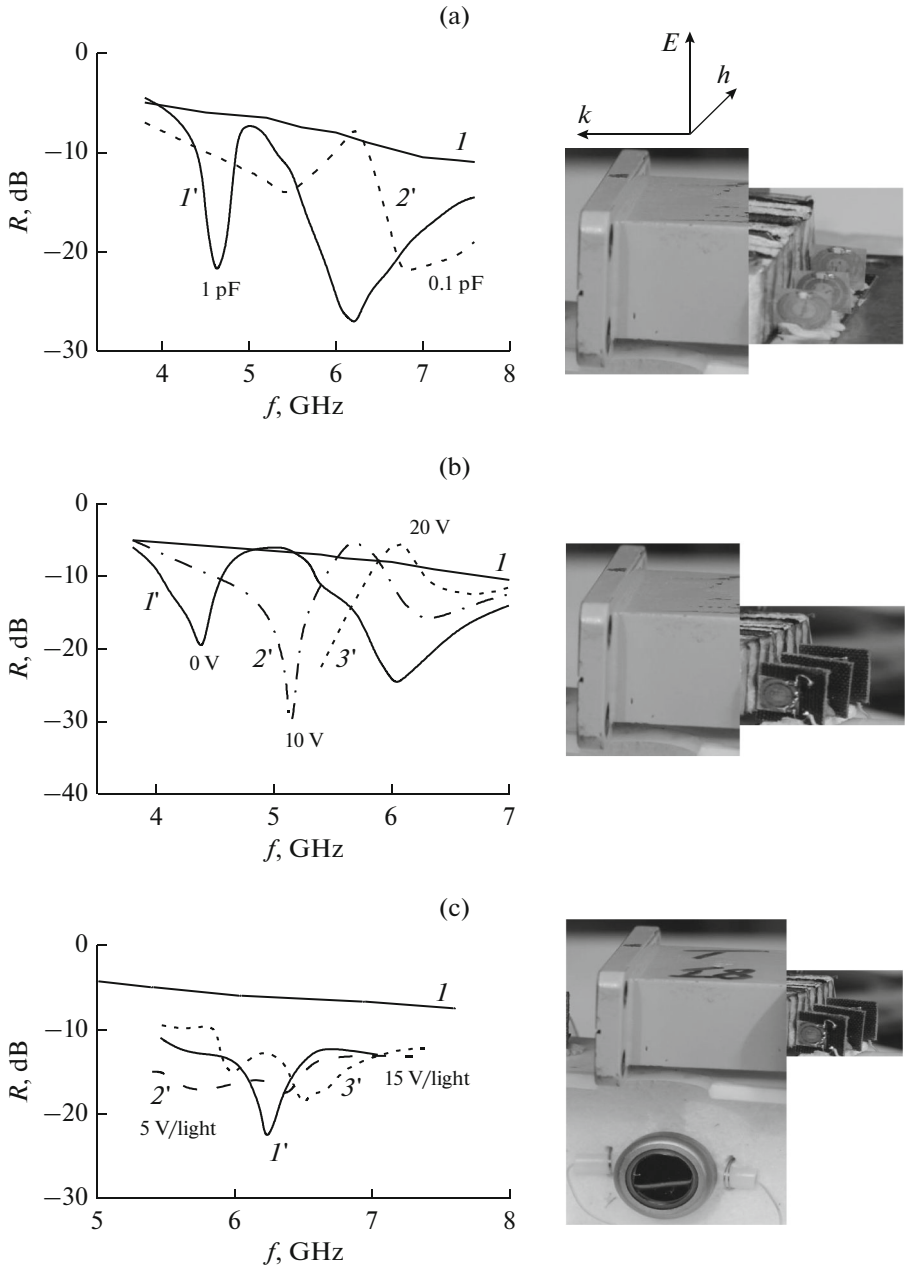

Fig. 7. Dynamics of the experimental frequency dependences of the reflection coefficient R from the radio-absorbing metastructure in the region of matching by means of three PDSRRs upon variation in the capacitance in an additional gap (*1*'–*3*') in comparison with R from (*1*) a free absorber: (a) capacitances of 0.1 and 1 pF; (b) varactor, V_{rb} = 0, 10, and 20 V (electrical control); (c) varactor/photodiode (optical control) (*1*') in the absence of light and under illumination of the photodiode at V_{rb} = (*2*') 5 and (*3*') 15 V.

controlled by means of a constant voltage or light have been developed. These metastructures contain a layered absorber and matching elements in the form of planar double-split-ring resonators with an additional gap in the outer ring, loaded with a MA46H120 (MACOM) varactor, or in the form of single twice-split-ring resonators with varactors in symmetrical gaps, and a magnetic resonance is supposed to be excited in them. On the basis of measurements in a rectangular waveguide and numerical calculations in free space, the dynamics of the frequency dependences of the reflection from the matching elements and the absorbing metastructures as the capacitances in the gaps are varied by means of external control has been studied. The electrical control is performed by applying a reverse bias voltage V_{rb} to the varactors, and

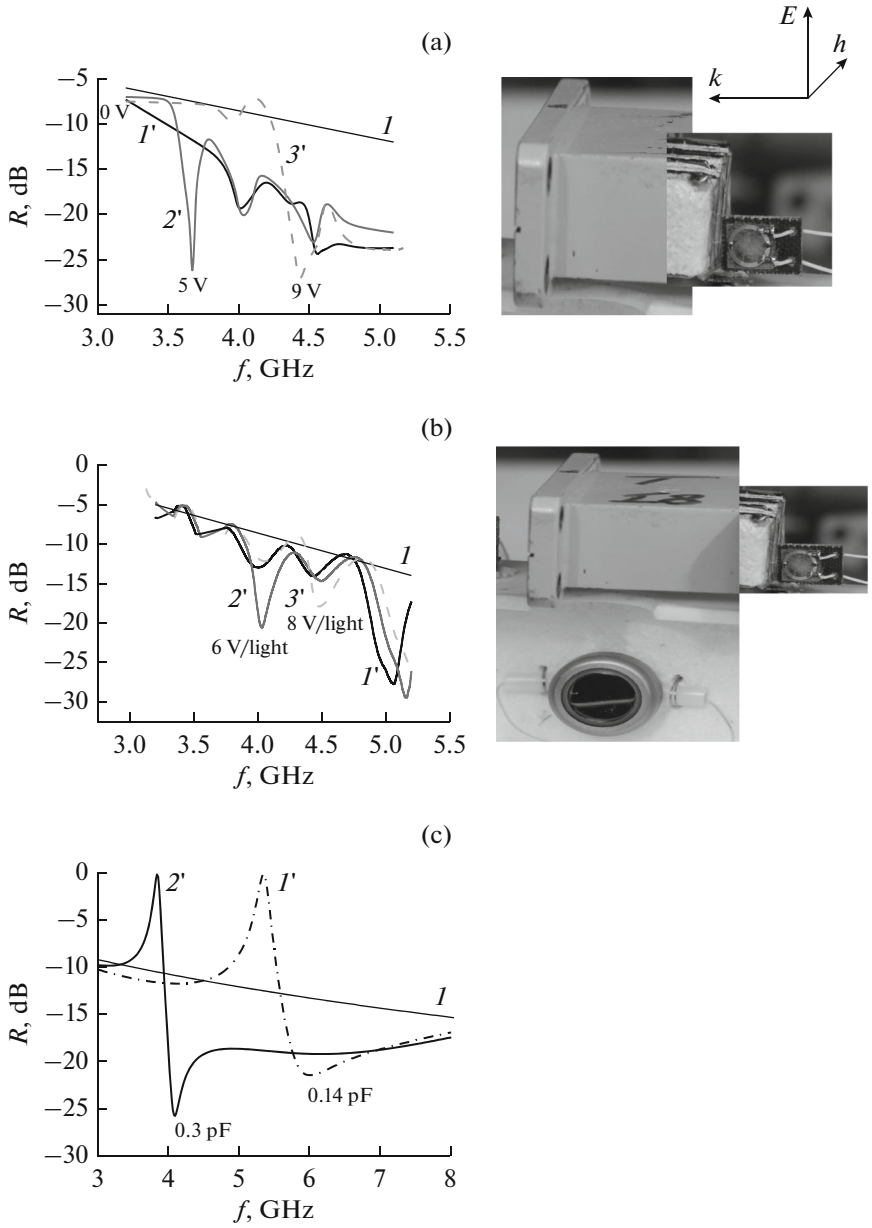

Fig. 8. Dynamics of (a, b) experimental and (c) calculated frequency dependences of the reflection coefficient R from a radio-absorbing metastructure in the region of matching using an STSRR upon variation in the capacitances (*1*'–*3*') in comparison with R from a free absorber: (a, curves *1*) electric control by means of varactors, $V_{rb} = 0$, 5, and 9 V; (b) optical control by means of combination of two varactors/photodiodes (*1*') in the absence of light and under illumination of the photodiode at $V_{rb} =$ (*2*') 6 and (*3*') 8 V; (c) the period of the array is 12 mm, and the permittivity of the absorber is $\varepsilon = 1 - j0.6 \times 10^{10}/f$.

the optical control, by turning on and off the light of a red laser pointer directed to the photodiode connected to the varactors in the photodiode mode.

The dynamics of reflection in the region of matching with the ambient space under electrical and optical control has been demonstrated by the comparison with a free absorber without matching elements. The tuning range of the reflection dips in the matching region is 25% with almost the same efficiency of electrical and optical control.

REFERENCES

1. V. K. Varadan, V. V. Varadan, and A. Lakhtakia, J. Wave-Mater. Interact. **2** (1), 71 (1987).
2. Ts. Songsong, V. A. Bannyi, A. L. Samofalov, et al., Probl. Fiz., Mat. Tekh., No. 4, 40 (2014).

3. M. Maasch, M. Schusler, E. Gonzalez Rodriguez, et al. in *Proc. 3rd Int. Congr. on Advanced Electromagn. Materials in Microwaves and Optics, 30 Aug.–4 Sept., London, 2009,* (Metamaterials'2009), p. 184.
4. Yu. N. Kazantsev, G. A. Kraftmakher, and V. P. Mal'tsev, J. Commun. Technol. Electron. **58**, 933 (2013).
5. G. A. Kraftmakher, V. S. Butylkin, and Yu. N. Kazantsev, Tech. Phys. Lett. **39**, 505 (2013).
6. G. A. Kraftmakher, V. S. Butylkin, and Yu. N. Kazantsev, Tech. Phys. Lett. **41**, 723 (2015).
7. H. K. Kim, D. Lee, and S. Lim, Appl. Opt. **55** (15), 4113 (2016). doi 10.1364/AO.55.004113
8. C. Mias, Electron. Lett. **39** (14), 1060 (2003).
9. J. Zhao, Q. Cheng, J. Chen, et al., New J. Phys. **15**, 043049 (2013).
10. B-Q. Lin, S-H. Zhao, Q-R. Zheng, et al., Progress in Electromagn. Res. **43**, 247 (2013).
11. Z. Luo, J. Long, X. Chen, and D. Sievenpiper, Appl. Phys. Lett. **109**, 071107 (2016). http://dx.doi.org/10.1063/1.4961367
12. B. Zhu, Y. J. Feng, J. M. Zhao, et al., Appl. Phys. Lett. **97**, 051906 (2010).
13. Yu. N. Kazantsev, G. A. Kraftmakher, and V. P. Mal'tsev, Tech. Phys. Lett. **42**, 238 (2016).
14. Yu. N. Kazantsev, G. A. Kraftmakher, and V. P. Mal'tsev, J. Commun. Technol. Electron. **61**, 614 (2016).
15. V. S. Butylkin and G. A. Kraftmakher, J. Commun. Technol. Electron. **53** (1), 1 (2008).
16. G. A. Kraftmakher, V. S. Butylkin, Yu. N. Kazantsev, et al., in *Proc. 7th Int. Conf. on Metamaterials, Photonic Crystals and Plasmonics (META'16), Malaga, Spain, July 25–28, (2016)* (META'**16**, 2016), p. 2060. http://www.metaconferences.org.
17. I. V. Shadrivov, P. V. Kapitanova, S. I. Maslovski, and Yu. S. Kivshar, Phys. Rev. Lett. **109**, 083902 (2012).

Translated by E. Chernokozhin